Ultrasound in Med. & Biol., Vol. 00, No. 00, pp. 1–11, 2022

0301-5629/$ - see front matter

https://doi.org/10.1016/j.ultrasmedbio.2022.05.019

● *Original Contribution*

BACTERICIDAL EFFECT OF ULTRASOUND-RESPONSIVE MICROBUBBLES AND SUB-INHIBITORY GENTAMICIN AGAINST *PSEUDOMONAS AERUGINOSA* BIOFILMS ON SUBSTRATES WITH DIFFERING ACOUSTIC IMPEDANCE

Filip Plazonic,[*,1] Gareth LuTheryn,[*,†,‡,1] Charlotte Hind,[§] Melanie Clifford,[§] Michael Gray,[¶] Eleanor Stride,[¶] Peter Glynne-Jones,[*] Martyn Hill,[*] J. Mark Sutton,[§,‖] and Dario Carugo[†]

* Faculty of Engineering and Physical Sciences, University of Southampton, Southampton, UK; † Department of Pharmaceutics, School of Pharmacy, University College London, London, UK; ‡ National Biofilms Innovation Centre, University of Southampton, Southampton, UK; § UK Health Security Agency, Porton Down, Salisbury, Wiltshire, UK; ¶ Institute of Biomedical Engineering, University of Oxford, Oxford, UK; and ‖ Institute of Pharmaceutical Science, King's College London, London, UK

(*Received* 9 *February* 2022; *revised* 10 *May* 2022; *in final form* 13 *May* 2022)

Abstract—The aim of this research was to explore the interaction between ultrasound-activated microbubbles (MBs) and *Pseudomonas aeruginosa* biofilms, specifically the effects of MB concentration, ultrasound exposure and substrate properties on bactericidal efficacy. Biofilms were grown using a Centre for Disease Control (CDC) bioreactor on polypropylene or stainless-steel coupons as acoustic analogues for soft and hard tissue, respectively. Biofilms were treated with different concentrations of phospholipid-shelled MBs (10^7–10^8 MB/mL), a sub-inhibitory concentration of gentamicin (4 μg/mL) and 1-MHz ultrasound with a continuous or pulsed (100-kHz pulse repetition frequency, 25% duty cycle, 0.5-MPa peak-to-peak pressure) wave. The effect of repeated ultrasound exposure with intervals of either 15- or 60-min was also investigated. With polypropylene coupons, the greatest bactericidal effect was achieved with 2 × 5 min of pulsed ultrasound separated by 60 min and a microbubble concentration of 5×10^7 MBs/mL. A 0.76 log (83%) additional reduction in the number of bacteria was achieved compared with the use of an antibiotic alone. With stainless-steel coupons, a 67% (0.46 log) reduction was obtained under the same exposure conditions, possibly due to enhancement of a standing wave field which inhibited MB penetration in the biofilm. These findings demonstrate the importance of treatment parameter selection in antimicrobial applications of MBs and ultrasound in different tissue environments. (E-mail addresses: D.Carugo@ucl.ac.uk, dario.carugo@gmail.com) **© 2022 The Author(s). Published by Elsevier Inc. on behalf of World Federation for Ultrasound in Medicine & Biology. This is an open access article under the CC BY license (http://creativecommons.org/licenses/by/4.0/).**

Key Words: **Ultrasound, Biofilm, Bacteria, Microbubble, Antibiotic, Antimicrobial resistance, Chronic wound, Substrate.**

INTRODUCTION

Bacterial biofilms present a serious threat to our ability to treat infections (Lebeaux et al. 2014). They can drastically reduce the effectiveness of antibiotics, primarily by inhibiting drug penetration (Singh et al. 2017). For a large proportion of bacteria inside the biofilm this means that the concentration of antibiotic that reaches them will not be high enough to kill them, which gives them greater opportunity to develop and express further resistance mechanisms. Combining antibiotics with drug delivery methods that increase their penetration and absorption capabilities thus has great potential to counteract this ever-growing threat to public health. Biofilms in chronic wounds are a key focus of research in this area, as they pose a significant risk of morbidity and even mortality. A chronic wound can be broadly classified as any wound that exhibits poor healing. These are typically associated with recalcitrant infections, ischemia and a prolonged or arrested inflammatory phase (Wolcott et al. 2008). Diabetic foot ulcers (DFUs) are a severe complication observed in 15% of neuropathic diabetic patients, making it one of the most prevalent examples of a chronic wound worldwide (Alexiadou and

Address correspondence to: Dario Carugo, Department of Pharmaceutics, School of Pharmacy, University College London, 29-39 Brunswick Square, London WC1N 1AX, UK.E-mail addresses: D.Carugo@ucl.ac.uk, dario.carugo@gmail.com

[1] Co-authors have made an equal contribution to this work.

Doupis 2012). There is a pronounced heterogeneity associated with bacterial colonisation of wounds, which has an intrinsic effect on morphology, mechanical properties and development of biofilms in chronic wounds (Thomson 2011). A comparative study of the foot microbiome revealed that, when compared with a non-diabetic foot, the diabetic foot was host to substantially more opportunistic pathogens such as *Staphylococcus aureus* and *Pseudomonas aeruginosa* (Jneid et al. 2017). Furthermore, it has been determined that a typical wound can consist of multiple genera, with 12−20 different aerobic and anaerobic species of pathogenic bacteria dominating the commensal microflora in some cases (Omar et al. 2017). Although studies have specifically implicated the microbial burden of DFUs in delayed wound healing (Attinger and Wolcott 2012; Bjarnsholt 2013), there must also be consideration of the species present in the pathophysiology of chronic wounds (Gardner et al. 2013). The experimental work carried out here has utilized a single-species *P. aeruginosa* biofilm, as it is an extensively used model organism for opportunistic Gram-negative infections (LaBauve and Wargo 2012) and is one of the most commonly isolated pathogens in chronic wounds (Banu et al. 2015).

The longest established method of biofilm eradication from chronic wounds is debridement (Yazdanpanah et al. 2015), which has been found to expedite wound healing and reduce the overall size of a wound (Rhoads et al. 2008). However, complete wound healing requires multiple invasive treatments, typically carried out over a period of months (Harris et al. 2018; Michailidis et al. 2018). Although the efficacy of debridement can be increased with the use of chemicals such as hydrogen peroxide or certain enzymes (Watters et al. 2016), failure to remove biofilm persister cells from the wound bed is a common cause of recalcitrance (Percival et al. 2011). A commonly overlooked requirement of debridement is the prolonged aftercare, including cleaning and redressing of the treated area over the course of weeks. In addition to the physical and emotional trauma associated with DFU management, there is an undeniable economic burden (Walsh et al. 2016). A recent cohort study by Guest et al. (2020) determined that the 2017/2018 annual cost of wound management to the UK National Health Service (NHS) was £8.3 billion. It is notable that of this, £5.6 billion was associated with the management of unhealed wounds. It is evident that the currently available therapeutic options for the treatment of biofilms in wounds are limited in their effectiveness.

A potential solution to this issue is the use of ultrasound-activated gas-filled microbubbles (MBs). The dynamic response of MBs to relatively low-intensity ultrasound can cause perturbation of the biofilm and potentiate the effect of administered antibiotics. The breadth of research surrounding the therapeutic use of ultrasound-activated MBs has been steadily expanding over the last decade (Unger et al. 2004; Sirsi and Borden 2009). However, the application of this treatment modality to bacterial biofilms has only more recently begun to see an increase in research focus. Although more extensively reviewed elsewhere (LuTheryn et al. 2019; Kooiman et al. 2020; Lattwein et al. 2020), the biophysical effects of oscillating MBs have been found to have a direct impact on biofilm architecture and permeability.

Since first being reported in 2011, it has been clearly demonstrated that the combination of ultrasound and MBs promotes bactericidal activity in both planktonic and biofilm cultures (Ikeda-Dantsuji et al. 2011). Cavitating MBs are known to cause the development of pores in the biofilm architecture, which inevitably enhances the permeability and thus susceptibility of biofilms to antibiotics (Zhu et al. 2014). These denoted "sonobactericide" studies are a continually growing area of essential research, which have reported on the effects of MB-driven microstreaming for biofilm removal (Kooiman et al. 2014) and the use of shock waves to drive antibiotic penetration and disrupt the biofilm architecture (Gnanadhas et al. 2015). Many studies on the effects of ultrasound and MBs for drug delivery in biofilms utilize substrates such as standard polystyrene tissue culture well plates and disks or glass coverslips (Han et al. 2007; Ronan et al. 2016). In some of these studies, the possibility of standing waves occurring accidentally because of ultrasound reflection in the apparatus has been noted (Lattwein et al. 2020). However, in this research, the intentional utilisation of an acoustically reflective substrate provides valuable insight into the potential for applying this methodology near hard surfaces, such as bone, *in vivo*, which are likely to elicit standing waves (Ferri et al. 2019). In summary, the aim of this research was to explore the interaction between ultrasound-activated MBs and *P. aeruginosa* biofilms to elucidate the effects of MB concentration, ultrasound exposure regimes and substrate acoustic properties on bactericidal efficacy.

METHODS

Biofilm-on-coupon system: Design rationale and construction

A compact system was designed to expose *P. aeruginosa* biofilms to a MB suspension and antibiotic solution, which can subsequently be exposed to an ultrasound field. Figure 1 illustrates both cross-sectional and exploded 3-D schematics of the system, which allows experiments to be performed with 2 mL of an antibiotic−MB formulation. To suppress reflected and standing waves from the

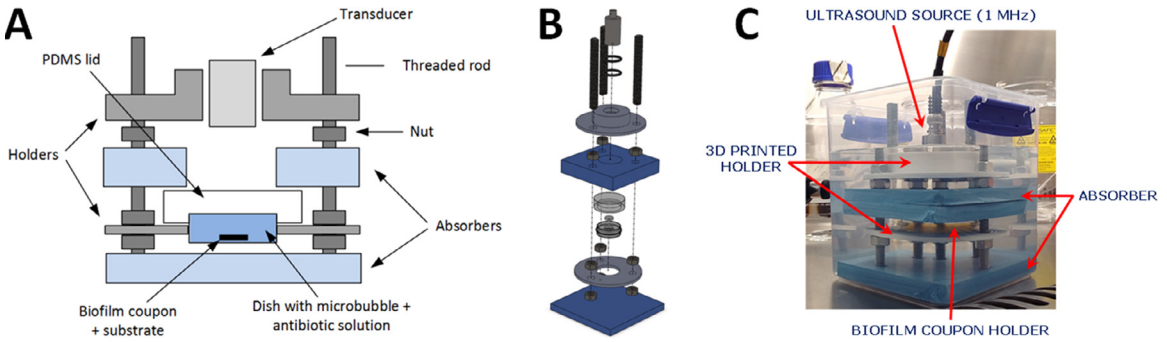

Fig. 1. (A) Schematic cross section and (B) expanded 3-D model of BOCS used to deliver ultrasound to a microbubble−antibiotic suspension, proximal to a biofilm grown on a polypropylene or stainless-steel Centre for Disease Control bioreactor coupon. The transducer and coupon holder are held in place by 3-D printed components, with a proprietary ultrasound-absorbing material lateral to the transducer and basal to the sample to prevent reflection of acoustic waves. The device components are all aligned using threaded steel rods and held in place with nuts. (C) Photograph of fully assembled BOCS within a compact water tank, with key features indicated (base 15 × 15 cm, and height of 20 cm). BOCS = biofilm-on-coupon system; PDMS = polydimethylsiloxane.

sidewalls and base of the biofilm-on-coupon system (BOCS), a layer of an acoustically absorbing material (Aptflex F48, 10 mm thick, Precision Acoustics, Dorchester, UK) was used. *Pseudomonas aeruginosa* biofilms were grown on Centre for Disease Control (CDC) bioreactor coupons, 12.7 mm in diameter and 3 mm thick, which were made of either polypropylene or stainless steel. A coupon holder was fabricated from an Ibidi dish with a polymer coverslip bottom (35 mm in diameter and 12 mm high; Ibidi, Martinsried, Germany). The volume of the dish was filled with a 10-mm-thick layer of polydimethylsiloxane (PDMS), which contained a 3-mm-deep recess to hold the coupon in a fixed position. After the coupon was placed in the recess of the holder, the dish was sealed with a removable 8-mm-thick PDMS lid, which was manufactured as described by Carugo et al. (2015). The lid also contained inlet and outlet ports for injection and removal of liquid samples, respectively. PDMS was selected for constructing the coupon holder and lid, as loss of transmission through this material layer at 1 MHz is low. Ultrasound is therefore able to pass through the lid and coupon holder without significant distortion (Carugo et al. 2015), to stimulate MBs and interact with the coupon substrate. The coupon holder and the transducer (1 MHz, narrowband, 15-mm-diameter active area, Camasonics, Wiltshire, UK) were held at a set distance of 40 mm by two 3-D-printed polylactic acid (PLA) mounting pieces, secured by nuts on three equidistant threaded rods.

Calibration of BOCS acoustic field

The acoustic pressure field was characterized using a needle hydrophone (2-mm-diameter needle, Precision Acoustics, Dorchester, UK), with the BOCS submerged in a tank filled with filtered and de-gassed water. To quantify the acoustic pressure field over specific regions of interest, automated position-control software (UMS2, Precision Acoustics, Dorchester, UK) was employed to control the hydrophone's position. Signals were acquired with an oscilloscope (Waverunner 64Xi, Teledyne LeCroy, Geneva, Switzerland). Drive voltage (PP007-WR, LeCroy) and current (4100, Pearson Electronics, Palo Alto, CA, USA) ultrasound probes were monitored to allow subsequent calculation of electrical impedance.

Calibration data were processed in MATLAB (version 7.10.0, The MathWorks, Natick, MA, USA) using the following steps: (i) application of a high pass filter to remove DC offset, (ii) calculation of the hydrophone's output sound intensity level $A(f,x,y,z)$ and drive voltage $V(f)$ Fourier transforms and (iii) calculation of the transmitting voltage response (TVR) at each frequency (f) and scan grid point (x,y,z): $\mathrm{TVR}(f,x,y,z) = A(f,x,y,z)/(V(f)\,S(f))$, where $S(f)$ is the hydrophone sensitivity given by manufacturer calibration. Water temperature was monitored with a glass thermometer, where resulting values were used to calculate the sound speed for use in estimating the hydrophone's position.

Two tests were performed: (i) the voltage dependence of the acoustic peak-to-peak pressure in the target plane at the transducer resonant frequency (1 MHz), to identify drive voltages able to create acoustic pressure amplitudes suitable for MB stimulation; and (2) a planar scan of the acoustic pressure in the target plane, to spatially characterize the ultrasound field to which bacteria and MBs were exposed. The target plane in this study corresponded to the location where biofilms were present; moreover, calibration tests were performed in the

presence of the PDMS lid to account for potential ultrasound attenuation through the lid.

Microbubble production protocol

The MB shell constituents were 1,2-distearoyl-*sn*-glycero-3-phosphocholine (DSPC) (850365P Avanti, Sigma-Aldrich, St. Louis, MO, USA) and polyoxyethylene (40) stearate (PEG40s) (P3440, Sigma-Aldrich). They were initially dissolved in chloroform at stock concentrations of 25 and 10 mg/mL, respectively, and were combined in a 9:1 or 9:5 molar ratio in a 20-mL-capacity, 23-mm-diameter glass vial (15394769, Fisherbrand, Fisher Scientific, Bellefonte, PA, USA), using a 1-mL Luer lock glass syringe (1MR-GT, S.G.E Gas Tight Syringe, Supelco). The lipid solution was covered with Parafilm that was pierced a number of times with a needle, then placed in a fume hood to allow the solvent to evaporate overnight at ambient temperature (~23 ± 2°C). The dry lipid film obtained was rehydrated with 5 mL of de-gassed 0.01 M sterile phosphate-buffered saline (PBS, P4417, Sigma-Aldrich), leaving a final lipid concentration of 4 mg/mL. A magnetic stirring bar was added to the vial before it was capped and placed on a stirring hotplate (Fisherbrand, Isotemp) for 30 min at 700 rpm and a temperature of 90°C (which is above the transition temperature for DSPC). Using a 120-W, 3.175-mm-diameter tip sonicator (20 kHz, Fisher Scientific FB120, Pittsburgh, PA, USA) the DSPC:PEG40s suspension was homogenously dispersed for 150 s at 40% power (48 W), with the sonicator tip fully immersed in the liquid. MBs were formed in a second sonication step by placing the tip sonicator at the liquid−air interface of the homogenized lipid suspension for 30 s at 70% power (84 W). Upon completion of the second sonication, the vial was placed immediately into an ice bath to rapidly cool the MB suspension. MBs were always prepared <3 h before being utilized in experiments and stored at ~4°C during the intervening period. The microbubble formulations investigated in the present study had an air-filled core. As this research ultimately aims to develop an ultrasound-mediated therapy for the topical treatment of infections in chronic wounds, it is anticipated that the stability of a microbubble formulation for this application would not suffer from the same challenges as for formulations administered intravenously, where microbubbles are exposed to greater temperatures and mechanical forces and can also be de-stabilized by their interaction with blood constituents. Moreover, whilst the diameter of microbubbles administered intravascularly should be less than ~10 μm to minimize the risk of microvascular occlusion (Stride and Saffari 2003), the size of microbubbles administered topically is not so constrained. Therefore, it was deemed suitable to initially evaluate the potential of a cost-effective air-filled formulation, as an alternative to heavier and less water-soluble gases that are more commonly used as the microbubble core constituent (such as sulfur hexafluoride and perfluorocarbons) (Qin et al. 2009).

Characterisation of microbubble stability

The stability of MBs stored at ~4°C was assessed by pipetting a 10-μL sample of the MB suspension onto a Neubauer hemocytometer, with a 0.17-mm-thick coverslip placed on top. By use of bright-field microscopy (IX71, Olympus, Tokyo, Japan) with a 50 × objective (LMPLFLN, Olympus), 100 images were acquired from randomly selected locations using a CCD camera (Hamamatsu ORCA-ER, C4742-80). The images were processed using ImageJ following a protocol previously reported (Schneider et al. 2012), and the process was repeated at intervals of 0, 1, 2, 5 and 24 h.

Biofilm growth

An overnight culture of *P. aeruginosa* (NCTC 13359) was prepared by inoculating three colonies into 3 mL of tryptone soy broth (TSB), which was then grown at 37°C with shaking at 200 rpm. The optical density (OD600) of the overnight culture was adjusted to a concentration of 1×10^8 CFU/mL, in a final volume of 2 mL. Biofilms were generated by inoculating 400 mL of sterile TSB with the 2 mL of adjusted *P. aeruginosa* culture, which was added to a sterile CDC bioreactor containing up to eight rods, each of which holds three 12.7-mm polypropylene or stainless-steel coupons. The top of the bioreactor was sealed with foil and placed on a stirring hotplate (Fisherbrand, Isotemp) at 37°C with a rotational speed of 200 rpm for 24 h.

Ultrasound-stimulated microbubbles for antibiotic delivery to P. aeruginosa *biofilms*

Pseudomonas aeruginosa biofilm-covered coupons were individually placed into the PDMS coupon holders using tweezers; controls that were exposed to antibiotic alone were handled in the same way but not exposed to MBs and/or ultrasound. A MB suspension was combined with a sub-inhibitory concentration of gentamicin (4 μg/mL final concentration) to attain an antibiotic:MB volumetric ratio of 1:1, 1:5 or 1:10. For experiments conducted in the absence of gentamicin, the MB suspension was diluted in the same volumetric ratios with sterile PBS. A 3-mL syringe (Thermo Scientific S7510-3) was used to draw up 2 mL of the antibiotic−microbubble (AB-MB) formulation and injected through the PDMS lid of the coupon holder dish. Injection was performed slowly at a 45° angle until no air spaces were visible in the dish; the inlet and outlet ports of the lid were then

sealed. The coupon holder was mounted onto the 3-D-printed holder and submerged in water in the fully assembled BOCS. Both sides of the bioreactor coupon were exposed to the same test parameters; these included either (i) a 15-min priming period with the AB−MB formulation before a single ultrasound exposure, or (ii) a 5-min priming period before an initial ultrasound exposure, followed by either a 15- or 60-min AB−MB priming period before a repeated ultrasound exposure. It was hypothesized that the introduction of a rest period between ultrasound exposures would provide time for the antibiotic to further diffuse through the biofilm, thus potentially enhancing the effect of the mechanical perturbation generated by MB cavitation. Moreover, previous studies on mammalian cell lines have reported on a priming effect caused by the constituents of lipid-based MB formulations, resulting in changes in cell membrane fluidity and permeability to bio-active compounds (Carugo et al. 2017; Aron et al. 2019). A maximum rest period of 60 min was selected in this study so as not to excessively prolong the overall duration of the treatment protocol, in view of potential future translation.

Both continuous and pulsed ultrasound exposure regimes were created using a signal generator (Rigol, DG1022A). The signal was fed to a power amplifier (55 dB gain, AG1020, T&C Power Conversion Inc., Rochester, NY, USA), which then output the signal to the transducer at 200 Vpp to create a 0.5-MPa peak-to-peak acoustic pressure amplitude at 1 MHz (see Fig. S1 [online only] for the acoustic field calibration data). The exposure time was 5 min, and for the pulsed exposures there was a 100-kHz pulse repetition frequency (PRF) at 25% duty cycle. These exposure conditions are comparable to those employed in previous *in vitro* studies reporting on the treatment of bacterial biofilms using combinations of US-activated microbubbles and antibiotics (He et al. 2011; Dong et al. 2013, 2017). During BOCS assembly in water, care was always taken to ensure that no exogenous air bubbles were trapped in the sound path. After ultrasound exposure, the coupon was removed from the holder and placed into a sterile bioreactor rod. The rods containing post-treatment coupons were stored upright in Falcon tubes containing 50 mL of sterile TSB and 4 μg/mL gentamicin, before being sealed with foil and incubated at 37˚C for 24 h.

After incubation, the viable cells from the biofilm were enumerated using the Miles−Misra method (Miles et al. 1938). To remove any residual planktonic cells from the coupons, each rod was washed by being gently rinsed in a Falcon tube containing 40 mL of sterile PBS. The coupons were then removed from the rod and individually placed into 15-mL Falcon tubes containing 10 mL of sterile TSB. To detach the biofilm from each coupon, the tubes were sealed and agitated at 2000 rpm for 10 min on a benchtop shaker. For each coupon, three 10-μL samples of the TSB containing extricated biofilm were taken; each sample was placed into 90 μL of sterile PBS on a 96-well plate and serially diluted to 10^{-8}. For each serial dilution, three 10-μL droplets were dispensed onto a sterile tryptone soy agar plate; the droplets were allowed to dry before the plate was inverted and incubated overnight at 37˚C. After incubation, all clearly visible individual colonies were counted; one dilution factor was selected for each coupon to scale the number of visible colonies to gain an estimate of the number of colony-forming units (CFU) per coupon.

Data analysis

To facilitate data analysis, biological repeats of experiments were normalized to the mean of the antibiotic-only control coupon. All data processing was carried out with MATLAB (version 7.10.0, The MathWorks Inc.). The values displayed on the graphs in Figures 2 and 3 are log reductions. This is a base-10 logarithm representation of the number of bacteria removed from the biofilm with respect to the antibiotic-only control (which achieved a 0.4 log reduction in the number of bacteria). It can be calculated as $LR = \log(N_B/N_A)$, where N_B represents the bacteria numbers before treatment and N_A represents bacteria numbers after treatment. A 1-log reduction represents a 10-fold decrease in bacteria numbers (*i.e.,* 90%), while a 2-log reduction represents a 100-fold reduction (*i.e.,* 99%). For a more in-depth statistical analysis of distribution and significance, each value of any tested condition was normalized with respect to the mean value of the antibiotic-only control. This includes other controls, as well as any tested condition. The data could thus all be pooled together and compared as distributions. Each coupon represented one sample. For each experimental condition, at least three independent bioreactors were employed, which means a minimum of 9 samples per condition tested. The Jarque−Bera normality test was carried out on the data distribution; it was determined that data did not follow a normal distribution but could instead be fit with an inverse exponential function. Therefore, significance between data distributions was assessed using the Mann−Whitney *U*-test (with a p value <0.01) instead of the more commonly used Student *t*-test. Because the AB−MB treatments were expected to perform better than the antibiotic-only control, a one-tailed version of the test was employed.

RESULTS AND DISCUSSION

Microbubble stability

The mean concentration of MBs at the time of production was 1.19×10^8 MBs/mL, which decreased to

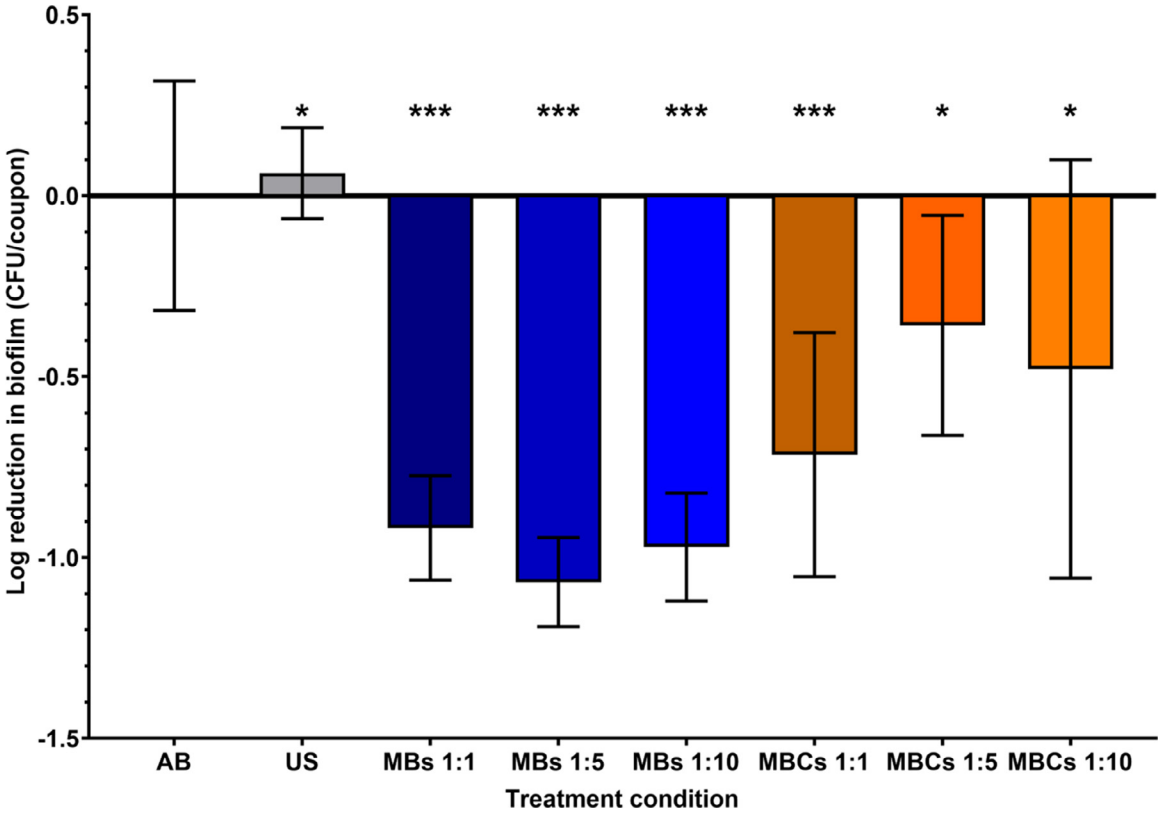

Fig. 2. Log reduction of numbers of bacteria for single-element controls, with AB only, US only, and MBs or MBCs alone in volumetric ratios of 1:1, 1:5 and 1:10 prepared in phosphate-buffered saline. Although the results indicate averaged data, it is important to note that all of the controls are compared with three coupons from the same bioreactor for the antibiotic control. To compare between bioreactors, the controls were normalized with respect to the antibiotic control, to determine the efficacy of the methodology against a sub-inhibitory concentration of antibiotic. The control experiments for sub-inhibitory gentamicin-only attained an average reduction in bacteria of 58% (0.4 log). Positive log values represent a reduction of bacterial cells, which under treatment conditions is achieved in addition to the baseline reduction established by the antibiotic alone. Negative log values compared with the AB-only control indicate continued bacterial growth after administration of MBs or MBCs to biofilms. The bubbles or constituents alone exhibit no significant bactericidal activity, and consequently post-exposure, the biofilm cells continue growing, and this results in a net increase in cells over time compared with an antibiotic treated control. Data are representative of three independent biological repeats, with error bars for standard deviations: $*p < 0.05$, $**p < 0.01$, $***p = 0.005$. AB = antibiotic; CFU = colony-forming units; MBs = microbubbles; MBCs = microbubble constituents; US = ultrasound.

5.97×10^7 MBs/mL in the 2-h interval before the experiment began. Over this time, the mean MB diameter increased from 2.9 ± 2.4 to 3.97 ± 4.1 μm. Assessment of MB concentration and diameter by microscopy was carried out at room temperature of approximately 20°C ($\pm$ 1°C), with the MB suspensions stored in an ice bath during the interim period. The size and concentration of MBs here are comparable to those of commercially available lipid-based MB preparations such as SonoVue, where post-production diameter and concentration are typically in the ranges $1.5-2.5$ μm and $1-5 \times 10^8$ MBs/mL, respectively (Sirsi and Borden 2009; Sennoga et al. 2012). As described earlier, air-filled microbubbles were investigated in this study as a potential US-responsive formulation for the topical treatment of biofilm infections. It should be noted that the measured increase in MB mean diameter over a 2-h period may be greater than that observed for similar lipid-shelled MB formulations containing less soluble gases (such as perfluorocarbons) (Pouliopoulos et al. 2020). This inevitably had an impact on the observed MB acoustic response, and further optimisation of the ultrasound exposure conditions—relative to the MB size distribution—could be carried out in future investigations. The observed reduction in MB concentration (and the corresponding increase in MB diameter) could be attributed to either gas diffusion from the MB core into the surrounding medium, leading to MB dissolution, or coalescence via Ostwald ripening. Both of these processes will typically be more pronounced for smaller MBs in a suspension, as their gaseous core is subject to greater pressure compared with

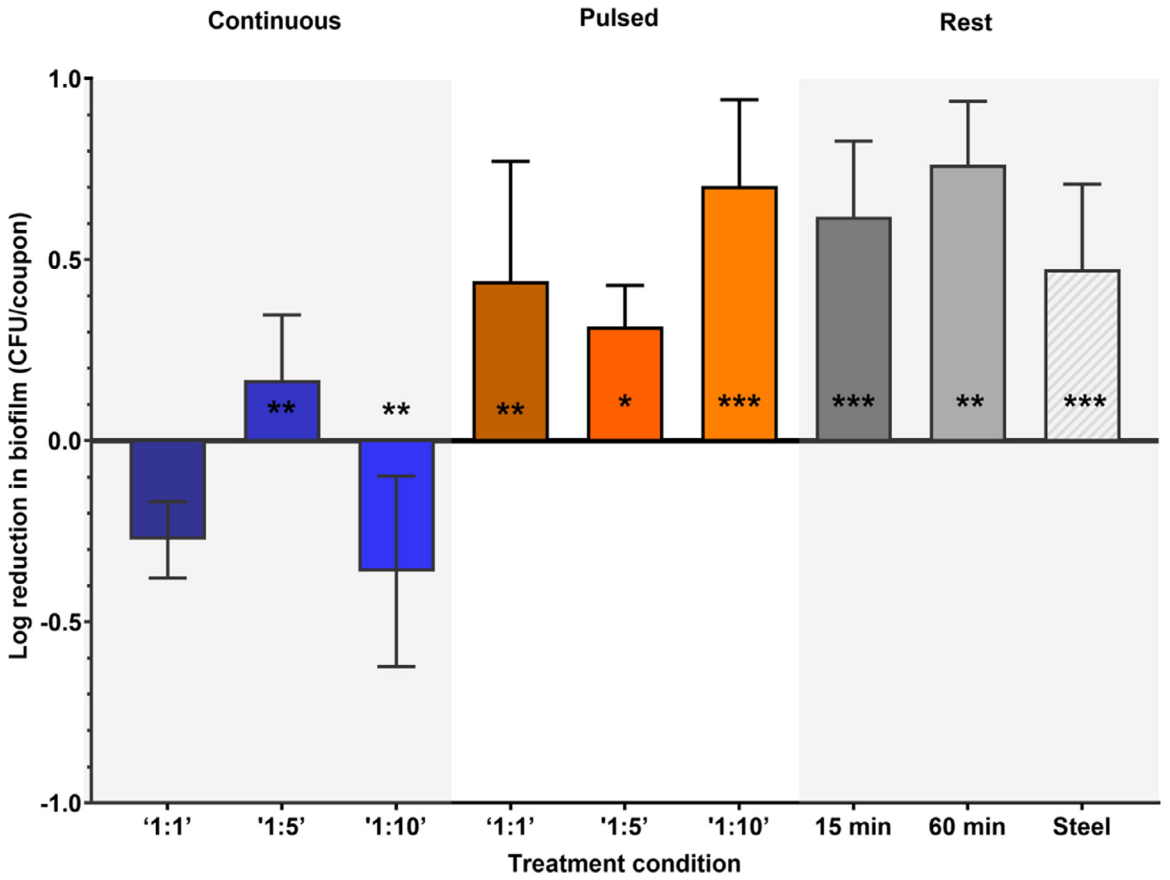

Fig. 3. Ultrasound was applied in both continuous wave (*left shaded area*) and pulsed wave (*centre unshaded area*), to AB−MB suspensions in volumetric ratios of 1:1, 1:5 and 1:10. The input voltage was 200 Vpp which produced a maximum peak-to-peak pressure of 0.5 MPa at the biofilm location. The frequency of the ultrasound was 1 MHz, and every exposure was 5 min long. In the case of pulsed ultrasound, the wave was pulsed at 25% duty cycle with a 100-kHz pulse repetition frequency. The *right shaded area* denoted as "rest" indicates the effect of adding a 15- or 60-min interval between the first and second sonications, using a 1:5 AB−MB suspension with pulsed wave. The final column labeled "steel" indicates the effect of a 1:1 AB−MB suspension with pulsed wave ultrasound and 15-min rest interval, but the polypropylene substrate has been exchanged for stainless steel. All data presented were compared with a sub-inhibitory gentamicin alone control (58%, 0.4 log), which was applied to biofilms without MBs or US. Specifically, data were normalized to the antibiotic-treated biofilm. For continuous wave US only, the 1:5 AB−MB suspension was able to attain a reduction in bacteria numbers, corresponding to an additional reduction of 32% (0.17 log) compared with the control. By use of pulsed wave US there was a consistent additional reduction in bacteria numbers compared with the control; for 1:1, 1:5 and 1:10, this corresponded to 64% (0.44 log), 52% (0.32 log) and 80% (0.7 log), respectively. The incorporation of a rest period between repeated pulsed wave ultrasound exposures revealed a further reduction of 76% (0.62 log) and 83% (0.76 log) for 15- and 60-min intervals, respectively. Changing the biofilm substrate to steel resulted in a 66% (0.47 log) additional reduction in bacteria numbers compared with the control. Data are representative of three independent biological repeats, with error bars for standard deviations. All conditions assessed with the exception of continuous wave ultrasound for a 1:1 AB−MB suspension were statistically significantly different from the sub-inhibitory antibiotic-alone control: $*p < 0.05$, $**p < 0.01$, $***p = 0.005$. AB = antibiotic; CFU = colony-forming units; MB = microbubble; US = ultrasound.

the larger MBs (because of surface tension and curvature effects) (Abou-Saleh et al. 2016; Epstein et al. 1950). The greater driving force for gas transport in smaller MBs is therefore a contributing factor behind the observed increase in mean MB diameter over time. Previous studies have also reported that MB dissolution time correlates inversely with gas diffusivity and solubility in the suspension medium, as well as gas permeability through the MB coating layer. This explains why air-filled lipid-shelled microbubbles undergo faster dissolution compared with those containing other clinically approved gases, such as perfluorocarbons and sulfur hexafluoride (Sarkar et al. 2009).

Experimental controls

To ensure the validity of control data for the biofilm samples, all coupons were subject to the same handling processes. The control conditions assessed included sub-inhibitory (4 μg/mL) antibiotic only, MBs only, MB shell constituents only and ultrasound only. The controls laid out here were important to establish if any bactericidal activity could be attributed to any single experimental condition, or if the treatment outcome was subject to a specific combination of parameters. The effect of MB shell constituents (MBCs) on biofilm samples was assessed, as previous research has indicated that constituents such as PEG have innate bactericidal properties (Shi et al. 2016; Owen et al. 2018).

To compare between bioreactors, the controls were normalized with respect to the antibiotic control to demonstrate the efficacy of the methodology using a sub-inhibitory concentration of antibiotic. Microbubble suspensions were separated into three volumetric ratios of PBS to MB of 1:1, 1:5 and 1:10. The same concentrations were used with the microbubble constituent controls. In the absence of ultrasound, MBs alone and MB constituents alone applied to biofilms did not exhibit any identifiable bactericidal or anti-biofilm activity when directly compared with antibiotic alone (Fig. 2). The investigated MB formulation and its constituents alone, at the concentrations tested, exhibited no significant bactericidal properties, and consequently post-exposure, the biofilm cells continue growing, resulting in a net increase in cells over time compared with an antibiotic-treated control. Similarly, in the absence of MBs, the ultrasound parameters alone had no effect on numbers of bacteria recovered from exposed biofilms (Fig. 2). In the ultrasound-only control, where no antibiotic or MBs were applied to the biofilm, there was a non-significant reduction in bacteria numbers equivalent to <23%.

Acoustic properties of substrates used for biofilm growth

To approximate acoustic exposure conditions of biofilms on soft tissues (such as skin) as well as proximal to hard tissues (such as bone), CDC bioreactor coupons were selected with contrasting acoustic impedance and speed of sound. As the range of materials that CDC bioreactor coupons are made from is limited, it was not possible to achieve a perfect match with tissue properties unfortunately, but the focus of the study was on the effect of a large difference in substrate properties. Polypropylene was chosen as a soft tissue analogue, as it facilitates efficient transmission. Soft tissues such as skin have a mean characteristic acoustic impedance of 1.63 MRayl, with a sound velocity of 1540 m/s and density of 1.06 g/cm^3 (Ludwig 2005). Polypropylene has a characteristic acoustic impedance of 2.36 MRayl, with a sound velocity of 2660 m/s and density of 0.89 g/cm^3 (ONDA Corp. 2003a). For modelling hard tissue, stainless-steel coupons were selected. Stainless steel has a much higher mean acoustic impedance (45.7 MRayl) than bone (7.71 MRayl) (Saïed et al. 2008); however, the sound velocity of bone is between 3700 and 4400 m/s (Sievänen et al. 2001) while that of stainless-steel is 5790 m/s (ONDA Corp. 2003b). Despite these differences in acoustic impedance and velocity, it was deemed that stainless-steel coupons would still provide valuable insight into the potential application of MBs proximal to highly acoustically reflective surfaces. In particular, it is anticipated that the more reflective steel coupon would favour the onset of a stronger ultrasonic standing wave field, and that the resulting acoustic radiation forces may potentially drive microbubbles away from the target surface and also cause microbubbles to aggregate (Lazarus et al. 2017; Jin et al. 2021). Differences in substrate properties may also have an impact on the amplitude of MB oscillation during cavitation and affect the probability and direction of resulting microjetting or microstreaming events. Moreover, differences in the pressure wave field within the solid substrate may cause additional convective effects at the solid−liquid interface, the characteristics of which would likely differ between polypropylene and stainless-steel substrates.

Continuous ultrasound exposure

A group of experiments explored the effect of bubble concentration on overall bacteria number reduction upon exposure to continuous-wave ultrasound (see the *left shaded area* in Fig. 3). In these experiments, biofilms were grown on polypropylene coupons. Only one of the three concentrations (1:5) was able to partially reduce bacteria numbers more than the antibiotic-only controls; however, although the change was statistically significant (p = 0.008), it does not represent a considerable reduction. The application of continuous-wave ultrasound to MBs in the context of achieving bactericidal or anti-biofilm activity is largely uncommon; as comprehensively reviewed by Lattwein et al. (2020), pulsed wave ultrasound is by far more common, likely because of the lower associated thermal effects compared with continuous-wave US fields. In a recent study by Fu et al. (2019) that utilized continuous-wave ultrasound (1 MHz, 3 W/cm^2, 5 min), an inhibitory effect of insonified MBs on *Acinetobacter baumannii* biofilms was reported to be more effective than that of antibiotic alone. However, this effect was discernibly less successful than those of other agents applied in the study to the same biofilms, confirmed in scanning electron microscopy images that revealed very little disruption to the biofilm architecture (Fu et al. 2019). The negligible effect of continuous-wave ultrasound and MBs applied in this research could be linked to MB concentration

within the confined space of the fluidic chamber where biofilms are contained. High-density MB clouds may scatter and absorb the incident ultrasound field and prevent it from pushing MBs to the biofilm surface, while at the same time creating a secondary shockwave if driven at the bubble cloud's resonance (Matsumoto and Yoshizawa 2005; Brujan et al. 2011). Consequently, this can create a complicated ultrasound−MB interaction, whereby a potential outcome is trapping and cavitation of MBs ineffectually away from the biofilm surface. Given the limited efficacy of MBs upon exposure to continuous-wave ultrasound, this treatment regime was not applied against biofilms grown on stainless-steel coupons.

Pulsed ultrasound exposure

In a second group of experiments (Fig. 3, *central unshaded area*), the effect of pulsing the ultrasound transducer (at 25% duty cycle) was evaluated. It was hypothesized that this would reduce aggregation and coalescence of MBs caused by secondary Bjerknes forces (Leighton 1997). Pulsing produced an overall improvement in bactericidal effect with all three MB concentrations. By use of a pulsed exposure, the greatest additional reduction in bacteria number was attained by an AB−MB suspension at a 1:10 ratio, which caused a substantial decrease in the number of bacteria (0.7 log, or 80%), with a significance of $p = 0.005$. The significant improvement in bactericidal efficacy of pulsed- over continuous-wave ultrasound in this research is promising, with strong evidence that pulsed-wave ultrasound and MBs have the ability to potentiate the effect of a sub-inhibitory concentration of antibiotic against biofilms. It has been reported that the synergy observed between pulsed-wave ultrasound and antibiotic potentiation is related to temporal peak intensity, rather than the temporal average intensity of the ultrasound (Cai et al. 2017). Consequently, as greater skin damage is correlated with higher average ultrasound intensities, the utilization of pulsed-wave ultrasound may prove essential in achieving clinically viable translations that utilize MBs and ultrasound for therapy.

Repeated ultrasound exposures after a rest period

As determined in other research, it is possible that repeated exposures to MBs and ultrasound can facilitate the opening of pores that expose deeper layers of the biofilm (Dong et al. 2013; Zhu et al. 2014). Consequently, when coupled with a prolonged rest period between ultrasound exposures, biofilm cells at deeper layers have time to be exposed to higher levels of oxygen, nutrients and antibiotic. This would invariably result in a greater level of metabolic activity in sessile cells that previously may have been dormant, which are renowned for being far more tolerant to antibiotic treatment (LuTheryn et al. 2019). Therefore, it is possible that additional exposures could reduce the numbers of bacteria even further, with each additional exposure increasing the time available for the antibiotic to penetrate and kill increasingly metabolically active cells. Adding a 15-min priming period prior to ultrasound exposure and a 15-min rest interval before a repeated exposure resulted in a significant improvement in treatment efficacy compared with antibiotic alone. The effect is illustrated here with the 1:5 AB−MB suspension, where the additional reduction in bacterial cells recovered from biofilms improved from 0.3 to 0.6 log (52%−76%), in the absence and presence of a rest period, respectively (Fig. 3). Moreover, when the rest interval between exposures was increased to 60 min, the reduction in number of bacteria was further increased to 0.76 log (83%) (Fig. 3, *right shaded area*). The significance of these tests was $p < 0.001$ (15-min rest period) and $p = 0.0095$ (60-min rest period). A similar result was obtained by Koibuchi et al. (2021), who explored the effect of continuous (1 MHz) and pulsed (1 MHz, 30 mW/cm^2, 20% duty cycle) ultrasound on *Staphylococcus epidermidis* biofilms in the absence of MBs. To obtain a similar inhibition of biofilm formation required 24 h of continuous irradiation, whilst pulsed wave achieved a significant reduction after two 20-min intervals. Importantly in this previous study it was found that, as in this research, the introduction of a second ultrasound exposure increased the treatment efficacy by almost double that of a single exposure (Koibuchi et al. 2021).

Effect of altering the acoustic properties of biofilm growth substrate

When polypropylene coupons were exchanged for stainless-steel ones, the reduction in viable count was lowered to only 0.5 log greater than that of the antibiotic alone ($p = 0.0009$) (Fig. 3, *right shaded area*). This is, however, still a significant improvement over using antibiotic alone. Given that stainless steel is an acoustically reflective substrate, it is inevitable that a stronger standing wave field is generated from the interaction between the incident and reflected waves (Baresch and Garbin 2020). The population of MBs will have a wide size distribution, such that some are pushed toward the pressure antinodes whilst others are pushed toward the nodes. At sub-resonance excitation conditions, MBs can be pushed by acoustic radiation forces toward the pressure nodes of a standing wave field (*i.e.,* away from a target surface) (LaBauve and Wargo 2012). At a mean MB size of 3.97 $\pm$ 4.1 μm (at the time of administration) with a resonant frequency of approximately 1 MHz, it is expected that the majority of MBs in this study would be pushed toward the pressure anti-node, which would be located

close to the surface of the steel coupon. However, clustering of MBs is very likely to occur, whereby the larger MB clusters could in turn be directed toward the pressure nodes (*i.e.,* away from the surface) (Lazarus et al. 2017). The behaviour of MBs in a standing wave field is therefore complex to characterize and may result in undefined MB dynamics (Wiklund 2012); it is a task for future studies to elucidate this further. Despite this, pulsed-wave ultrasound applied to biofilms grown on stainless steel was still approximately 67% (0.47 log) more effective when compared with use of antibiotic alone (Fig. 3).

CONCLUSIONS

This research has illustrated the efficacy of ultrasound and air-filled MBs to potentiate the effect of sub-inhibitory concentrations of antibiotic against *P. aeruginosa* biofilms grown on substrates with physiologically relevant acoustic properties. Importantly, this work indicates the utility of this method in being adapted to coincide with clinical treatment time scales, where the minimally invasive administration of ultrasound and MBs could achieve a reduction in biofilm bacteria of 80% in approximately 60 min or less. The efficacy of this method was found to be reduced when applied to biofilms on highly acoustically reflective substrates, potentially because of the formation of a stronger acoustic standing wave field. Further study is required in this area to elucidate these phenomena in greater detail. The results from this study suggest that ultrasound and microbubbles provide improvements over more traditional methods of biofilm treatment, by enabling sub-inhibitory antibiotic concentrations to attain an equal or better level of bactericidal activity despite interactions with acoustically attenuating substrates. For such a method to become clinically viable in the future, the treatment efficacy should be improved further to achieve a reduction in viable bacterial cells of at least 3 log (*i.e.,* 99.9%). This may be attained by optimising the ultrasound exposure parameters and/or utilising microbubbles with greater stability, such as those containing gases with lower diffusivity and solubility.

With further optimisation and development, this approach may contribute toward reducing the overall clinical burden imposed by the presence of biofilms and lowering the impact of antimicrobial resistance. Furthermore, the local and topical administration of antimicrobial agents that can be potentiated with this method has potential to eliminate the need for long-term systemic antimicrobial therapy, which can have additional negative clinical outcomes consequences for patient health and recovery.

Acknowledgments—We thank the Engineering and Physical Sciences Research Council (EPSRC)−funded Network for Antimicrobial Resistance and Infection Prevention (NAMRIP, EP/M027260/1) and the ESPRC Programme Grant "Beyond Antibiotics" (EP/V026623/1) for funding this research.

Conflict of interest disclosure—The authors have no conflicts of interest to declare.

SUPPLEMENTARY MATERIALS

Supplementary material associated with this article can be found in the online version at doi:10.1016/j.ultrasmedbio.2022.05.019.

REFERENCES

Abou-Saleh RH, Peyman SA, Johnson BRG, Marston G, Ingram N, Bushby R, Coletta PL, Markham AF, Evans SD. The influence of intercalating perfluorohexane into lipid shells on nano and microbubble stability. Soft Matter 2016;12:7223–7230.

Alexiadou K, Doupis J. Management of diabetic foot ulcers. Diabetes Ther 2012;3:4.

Aron M, Vince O, Gray M, Mannaris C, Stride E. Investigating the role of lipid transfer in microbubble-mediated drug delivery. Langmuir 2019;35:13205–13215.

Attinger C, Wolcott R. Clinically addressing biofilm in chronic wounds. Adv Wound Care 2012;1:127–132.

Banu A, Hassan MMN, Rajkumar J, Srinivasa S. Spectrum of bacteria associated with diabetic foot ulcer and biofilm formation: A prospective study. Australas Med J 2015;8:280–285.

Baresch D, Garbin V. Acoustic trapping of microbubbles in complex environments and controlled payload release. Proc Natl Acad Sci USA 2020;117:15490–15496.

Bjarnsholt T. The role of bacterial biofilms in chronic infections. APMIS Suppl 2013;121:1–51.

Brujan EA, Ikeda T, Yoshinaka K, Matsumoto Y. The final stage of the collapse of a cloud of bubbles close to a rigid boundary. Ultrason Sonochem 2011;18:59–64.

Cai Y, Wang J, Liu X, Wang R, Xia L. A review of the combination therapy of low frequency ultrasound with antibiotics. BioMed Res Int 2017;2017 2317846.

Carugo D, Owen J, Crake C, Lee JY, Stride E. Biologically and acoustically compatible chamber for studying ultrasound-mediated delivery of therapeutic compounds. Ultrasound Med Biol 2015;41:1927–1937.

Carugo D, Aron M, Sezgin E, Bernardino de la Serna J, Kuimova MK, Eggeling C, Stride E. Modulation of the molecular arrangement in artificial and biological membranes by phospholipid-shelled microbubbles. Biomaterials 2017;113:105–117.

Dong Y, Chen S, Wang Z, Peng N, Yu J. Synergy of ultrasound microbubbles and vancomycin against *Staphylococcus epidermidis* biofilm. J Antimicrobial Chemother 2013;68:816–826.

Dong Y, Xu Y, Li P, Wang C, Cao Y, Yu J. Antibiofilm effect of ultrasound combined with microbubbles against *Staphylococcus epidermidis* biofilm. Int J Med Microbiol 2017;307:321–328.

Epstein PS, Plesset MS. On the Stability of Gas Bubbles in Liquid−Gas Solutions. J Chem Phys 1950;18:1505.

Ferri S, Polydorou A, May J, Wu Q, Stride EP, Evans ND, Carugo D. A physical model to investigate the acoustic behaviour of microbubbles and nanodroplets within a bone fracture. J Acoust Soc Am 2019;146:2775.

Fu YY, Zhang L, Yang Y, Liu W, He YN, Li P, Yu X. Synergistic antibacterial effect of ultrasound microbubbles combined with chitosan-modified polymyxin B-loaded liposomes on biofilm-producing *Acinetobacter baumannii*. Int J Nanomed 2019;1805–1815.

Gardner SE, Hillis SL, Heilmann K, Segre JA, Grice EA. The neuropathic diabetic foot ulcer microbiome is associated with clinical factors. Diabetes 2013;62:923–930.

Gnanadhas DP, Elango M, Janardhanraj S, Srinandan CS, Datey A, Strugnell RA, Gopalan J, Chakravortty D. Successful treatment of

biofilm infections using shock waves combined with antibiotic therapy. Sci Rep 2015;5:17440.

Guest JF, Fuller GW, Vowden P. Cohort study evaluating the burden of wounds to the UK's National Health Service in 2017/2018: Update from 2012/2013. BMJ 2020;10:45253.

Han YW, Ikegami A, Chung P, Zhang L, Deng CX. Sonoporation is an efficient tool for intracellular fluorescent dextran delivery and one-step double-crossover mutant construction in *Fusobactenum nucleatum*. Appl Environ Microbiol 2007;73:3677–3683.

Harris C, Coutts P, Raizman R, Grady N. Sharp wound debridement: Patient selection and perspectives. Chronic Wound Care Manage Res 2018;5:29–36.

He N, Hu J, Liu H, Zhu T, Huang B, Wang X, Wu Y, Wang W, Qu D. Enhancement of vancomycin activity against biofilms by using ultrasound-targeted microbubble destruction. Antimicrobial Agents Chemother 2011;55:5331–5337.

Ikeda-Dantsuji Y, Feril LB, Tachibana K, Ogawa K, Endo H, Harada Y, Suzuki R, Maruyama K. Synergistic effect of ultrasound and antibiotics against *Chlamydia trachomatis*-infected human epithelial cells in vitro. Ultrason Sonochem 2011;18:425–430.

Jin L, Wang W, Tu Y, Zhang K, Lv Z. Effect of ultrasonic standing waves on flotation bubbles. Ultrason Sonochem 2021;73 105459.

Jneid J, Lavigne JP, la Scola B, Cassir N. The diabetic foot microbiota: A review. Hum Microbiome J 2017;56:1–6.

Koibuchi H, Fujii Y, Sato'o Y, Mochizuki T, Yamada T, Cui L, Taniguchi N. Inhibitory effects of ultrasound irradiation on *Staphylococcus epidermidis* biofilm. J Med Ultrason 2021;48:439–448.

Kooiman K, Vos HJ, Versluis M, de Jong N. Acoustic behavior of microbubbles and implications for drug delivery. Adv Drug Deliv Rev 2014;72:28–48.

Kooiman K, Roovers S, Langeveld SAG, Kleven RT, Dewitte H, O'Reilly MA, Escoffre JM, Bouakaz A, Verweij MD, Hynynen K, Lentacker I, Stride E, Holland CK. Ultrasound-responsive cavitation nuclei for therapy and drug delivery. Ultrasound Med Biol 2020;46:1296–1325.

LaBauve AE, Wargo MJ. Growth and laboratory maintenance of *Pseudomonas aeruginosa*. Curr Protoc Microbiol 2012;25 6E.1.1−6E.1.8.

Lattwein KR, Shekhar H, Kouijzer JJP, van Wamel WJB, Holland CK, Kooiman K. Sonobactericide: An emerging treatment strategy for bacterial infections. Ultrasound Med Biol 2020;46:193–215.

Lazarus C, Pouliopoulos AN, Tinguely M, Garbin V, Choi JJ. Clustering dynamics of microbubbles exposed to low-pressure 1-MHz ultrasound. J Acoust Soc Am 2017;142:3135.

Lebeaux D, Ghigo JM, Beloin C. Biofilm-related infections: Bridging the gap between clinical management and fundamental aspects of recalcitrance toward antibiotics. Microbiol Mol Biol Rev 2014;78:510–543.

Leighton TG. The acoustic bubble. London: Academic Press; 1997.

Ludwig GD. The velocity of sound through tissues and the acoustic impedance of tissues. J Acoust Soc Am 2005;22:862.

LuTheryn G, Glynne-Jones P, Webb JS, Carugo D. Ultrasound-mediated therapies for the treatment of biofilms in chronic wounds: A review of present knowledge. Microb Biotechnol 2019;13:613–628.

Matsumoto Y, Yoshizawa S. Behaviour of a bubble cluster in an ultrasound field. Int J Numer Methods Fluids 2005;47:591–601.

Michailidis L, Bergin SM, Haines TP, Williams CM. Healing rates in diabetes-related foot ulcers using low frequency ultrasonic debridement versus non-surgical sharps debridement: A randomised controlled trial. BMC Res Notes 2018;11:732.

Miles AA, Misra SS, Irwin JO. The estimation of the bactericidal power of the blood. J Hyg (Lond) 1938;38:732–749.

Omar A, Wright JB, Schultz G, Burrell R, Nadworny P. Microbial biofilms and chronic wounds. Microorganisms 2017;5:9.

ONDA Corporation. Acoustic properties of plastics reference material; 2003a. Available at: https://www.ondacorp.com/images/Plastics.pdf. Accessed October 25, 2021.

ONDA Corporation. Acoustic properties of solids reference material; 2003b. Available at: https://www.ondacorp.com/images/Solids.pdf. Accessed October 25, 2021.

Owen J, Kamila S, Shrivastava S, Carugo D, de la Serna JB, Mannaris C, Pereno V, Browning R, Beguin E, McHale AP, Callan JF, Stride E. The Role of PEG-40-stearate in the Production, Morphology, and Stability of Microbubbles. Langmuir 2019;35:10014–10024.

Percival SL, Hill KE, Malic S, Thomas DW, Williams DW. Antimicrobial tolerance and the significance of persister cells in recalcitrant chronic wound biofilms. Wound Repair Regen 2011;19:1–9.

Pouliopoulos AN, Jimenez DA, Frank A, Robertson A, Zhang L, Kline-Schoder AR, Bhaskar V, Harpale M, Caso E, Papapanou N, Anderson R, Li R, Konofagou EE. Temporal stability of lipid-shelled microbubbles during acoustically-mediated blood−brain barrier opening. Front Phys 2020;8:137.

Qin S, Caskey CF, Ferrara KW. Ultrasound contrast microbubbles in imaging and therapy: Physical principles and engineering. Phys Med Biol 2009;54:R27.

Rhoads DD, Wolcott RD, Percival SL. Biofilms in wounds: Management strategies. J Wound Care 2008;17:502–508.

Ronan E, Edjiu N, Kroukamp O, Wolfaardt G, Karshafian R. USMB-induced synergistic enhancement of aminoglycoside antibiotics in biofilms. Ultrasonics 2016;69:182–190.

Saïed A, Raum K, Leguerney I, Laugier P. Spatial distribution of anisotropic acoustic impedance assessed by time-resolved 50-MHz scanning acoustic microscopy and its relation to porosity in human cortical bone. Bone 2008;43:187–194.

Sarkar K, Katiyar A, Jain P. Growth and dissolution of an encapsulated contrast microbubble: Effects of encapsulation permeability. Ultrasound Med Biol 2009;35:1385–1396.

Schneider CA, Rasband WS, Eliceiri KW. NIH Image to ImageJ: 25 years of image analysis. Nat Methods 2012;9:671–675.

Sennoga CA, Yeh JSM, Alter J, Stride E, Nihoyannopoulos P, Seddon JM, Haskard DO, Hajnal JV, Tang MX, Eckersley RJ. Evaluation of methods for sizing and counting of ultrasound contrast agents. Ultrasound Med Biol 2012;38:834–845.

Shi H, Liu H, Luan S, Shi D, Yan S, Liu C, Li RKY, Yin J. Effect of polyethylene glycol on the antibacterial properties of polyurethane/carbon nanotube electrospun nanofibers. RSC Adv 2016;6:19238–19244.

Sievänen H, Cheng S, Ollikainen S, Uusi-Rasi K. Ultrasound velocity and cortical bone characteristics in vivo. Osteoporos Int 2001;12:399–405.

Singh S, Singh SK, Chowdhury I, Singh R. Understanding the mechanism of bacterial biofilms resistance to antimicrobial agents. Open Microbiol J 2017;11:53–62.

Sirsi S, Borden M. Microbubble compositions, properties and biomedical applications. Bubble Sci Eng Technol 2009;1:3–17.

Stride E, Saffari N. Microbubble ultrasound contrast agents: A review. Proc Inst Mech Eng Part H 2003;217:429–447.

Thomson CH. Biofilms: Do they affect wound healing?. Int Wound J 2011;8:63–67.

Unger EC, Porter T, Culp W, Labell R, Matsunaga T, Zutshi R. Therapeutic applications of lipid-coated microbubbles. Adv Drug Deliv Rev 2004;56:1291–1314.

Walsh JW, Hoffstad OJ, Sullivan MO, Margolis DJ. Association of diabetic foot ulcer and death in a population-based cohort from the United Kingdom. Diabet Med 2016;33:1493–1498.

Watters CM, Burton T, Kirui DK, Millenbaugh NJ. Enzymatic degradation of in vitro *Staphylococcus aureus* biofilms supplemented with human plasma. Infect Drug Resist 2016;9:71–78.

Wiklund M. Acoustofluidics 12: Biocompatibility and cell viability in microfluidic acoustic resonators. Lab Chip 2012;12:2018–2028.

Wolcott RD, Rhoads DD, Dowd SE. Biofilms and chronic wound inflammation. J Wound Care 2008;17:333–341.

Yazdanpanah L, Nasiri M, Adarvishi S. Literature review on the management of diabetic foot ulcer. World J Diabetes 2015;6:37–53.

Zhu HX, Cai XZ, Shi ZL, Hu B, Yan SG. Microbubble-mediated ultrasound enhances the lethal effect of gentamicin on planktonic *Escherichia coli*. BioMed Res Int 2014;2014 142168.